

Design of Vehicle On-Glass Diversity Antennas for WiBro Applications

Seungbeom Ahn^{*(1)}, Yongsoo Cho⁽²⁾, and Hosung Choo⁽¹⁾

⁽¹⁾School of Electronic and Electrical Engineering, Hongik University
72-1 Sangsu-dong, Mapo-gu, Seoul, 121-791, Korea

⁽²⁾Dept. of Electronic Engineering, Chung-Ang University
221 Heukseok-dong, Dongjak-gu, Seoul, 156-756, Korea

Abstract—We propose diversity on-glass antennas with broad bandwidth, high radiation gain, and low surface area for WiBro internet applications. Triangular shaped patch was used as an individual antenna structure and the feeding locations of each antenna were varied so as to increase a channel capacity. The proposed antennas showed a -10 dB matching bandwidth of 11 % and a radiation gain of -6 dBi in the entire WiBro band. The correlation coefficient among four antennas using the measured WiBro signal strength showed less than 0.4.

I. INTRODUCTION

Recently, mobile internet services such as wireless fidelity (Wi-Fi), high speed downlink packet access (HSDPA), and wireless broadband (WiBro) have been launched in Korea. WiBro, also known as the international standard IEEE 802.16e, in particular achieves high data rates (up link: 5.2 Mbps, down link: 24.8 Mbps) and good mobility characteristics so that some vehicle manufacturers are attempting to install it in a new vehicle [1]. The internal WiBro system in vehicles generally uses monopole-type antennas such as simple whips in the vicinity of the WiBro transceiver near the front audio control box. These antennas, however, have relatively low radiation gain due to the body blockage effect of the vehicle. To mitigate this problem, on-glass antennas that are directly printed on a vehicle's windows can be employed [2-3]. In addition, diversity on-glass antennas that incorporate several printed antennas on a single window can be used to improve receiving performance [4].

This paper proposes an on-glass WiBro diversity antenna that maximizes a channel capacity. For the basic structure of the individual antenna body, we used a planar triangular patch to step-up the low input resistance of the on-glass antennas.

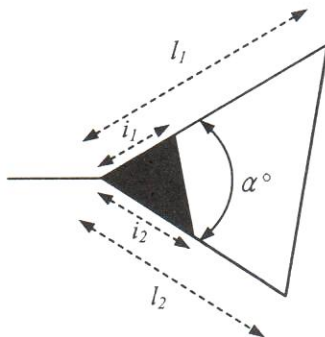


Figure 1. Configuration of the proposed antenna.

Inside the triangular patch was partly removed so the drivers' field of view was as unobstructed as possible. To obtain a maximum channel capacity, the feeding locations of four antennas were varied. Each antenna can be placed at the left, right, and upper sides of the rear window. To accurately obtain the 3D-radiation pattern of each antenna, the entire vehicular structure and the antenna body were inserted into the EM simulator (FEKO of *EM software and systems*). Correlation coefficients among the four antennas were calculated from 3D-radiation patterns, and an ergodic channel capacity of the Rayleigh channel that represents the flat-fading channel in urban environments, was obtained using the correlation coefficients [5]. The proposed antennas were mounted on the optimal locations of the rear window of a sedan, and the antenna characteristics, such as the matching bandwidth and radiation pattern, were measured in a semi-anechoic chamber. To confirm the diversity performance, we also measured the received power of the proposed antenna in the WiBro service zone, which revealed low correlation coefficients of 0.39 between the received signals from the individual antenna.

II. DESIGN METHODOLOGY AND RESULTS

Fig. 1 shows the proposed individual antenna geometry and the design parameters. Generally, on-glass antennas have very low input resistance because they are placed in close proximity to the conducting frame of vehicles. To increase the low input resistance of the antenna, we employed a planar triangular shape as the main antenna body because input resistance is dependent on the flare angle of triangular patch [6]. Also, the inside of the triangular patch was partially

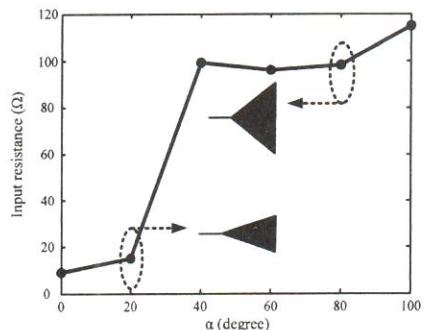


Figure 2. The input resistance by the flare angle α

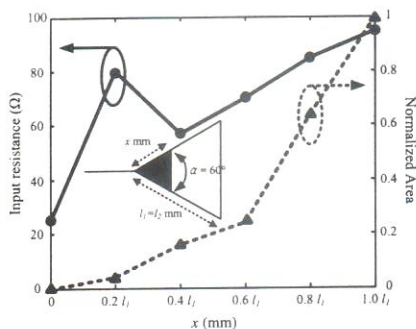


Figure 3. The input resistance by the surface area.

removed to broaden drivers' field of view. Fig. 2 shows a variation of input resistance depending on the flare angle α . As the angle α increases, the input resistance of the antenna also increases. Thus, to match with 50 Ω coaxial cable, the flare angle α should be greater than 40°. We also examined the variation of the input resistance depending on the filled area of the triangular patch as shown in Fig. 3. The side lengths of the outer triangular patch and the flare angle α are fixed as $l_1 = l_2 = 50$ mm and $\alpha = 60^\circ$. The length of the inner patch x is then gradually increased. In the figure, the normalized area is defined by the ratio of the inner filled area to the total triangular patch. The input resistance of the proposed antenna increases when x is enlarged. Considering the input resistance and drivers' field of view, appropriate lengths of the inner patch should be decided approximately as in between $0.2l_1$ and $0.6l_1$.

To obtain optimal the antenna performance, such as the broad impedance matching, high radiation gain, and low filled surface area, the design parameters were determined using a Pareto genetic algorithm (PGA) [7]. In the PGA optimization process, the final design goal was defined as:

$$\begin{aligned} \text{fitness 1} &= \min \{S_{11}(f_j)\} \\ \text{fitness 2} &= \max \left[\frac{1}{N \cdot M} \sum_{i=1}^N \sum_{j=1}^M \{G_{\text{ain}}(\phi_i, f_j)\} \right] \\ &\text{where } \begin{cases} \phi_i = 0 \sim 360^\circ, \theta = 90^\circ \\ 2.30 \text{ GHz} \leq f_j \leq 2.40 \text{ GHz} \end{cases} \\ \text{fitness 3} &= \min \left\{ \text{filled surface area} \left(\frac{i_1 \times i_2}{l_1 \times l_2} \right) \right\} \end{aligned} \quad (1)$$

The optimized design parameters are listed in Table I.

Based on the determined individual antenna structure, we examined the available channel capacity depending on the locations of each antenna in the rear window. Each antenna can be placed at the left, right, and upper sides of the rear window. Then, the 3D-radiation pattern of each antenna from the EM simulation, which includes the full vehicle body, was obtained to calculate the correlation coefficients among the four antennas. Equation (2) is the formula for calculating the correlation coefficient from 3D-radiation patterns. $A_i(\Omega)$ and $A_j(\Omega)$ are 3D-radiation patterns of the individual antennas i

TABLE I
DIMENSIONS OF THE OPTIMIZED ANTENNA

Parameter	α	l_1	l_2	i_1	i_2
Size	60°	41 mm	41 mm	10.25 mm	14.35 mm

$$\psi_{ij} = \frac{1}{\sigma_i \sigma_j} \oint E \left\{ (A_i(\Omega) \cdot E(\Omega)) (A_j^*(\Omega) \cdot E^*(\Omega)) \right\} d\Omega \quad (2)$$

and j , and $E(\Omega)$ is a random incident field. σ is the variance of the multiplication between the $A_i(\Omega)$ and $E(\Omega)$ [8]. Based on the correlation coefficient between the four antennas, we calculated the ergodic channel capacity using (3).

$$C = E \left\{ \log_2 \left[\det \left(I_{n_T} + \frac{\rho}{n_T} \tilde{H} \Psi \tilde{H}^T \right) \right] \right\} \quad (3)$$

where n_T and n_R are the numbers of transmitting and receiving antennas, \tilde{H} is an $n_T \times n_R$ normalized transfer matrix in a flat-fading channel, and ρ is a signal to noise ratio. The resulting channel capacity shows a maximum of 11.04 bps/Hz ($n_T = n_R = 4$, $\rho = -10$ dB), when the two antennas are placed at the left and right sides of the window frame, and the other two antennas are placed at the upper side of the window frame.

The proposed antennas were built and mounted at the optimal locations of the commercial sedan's rear window. Antenna characteristics, such as matching bandwidth and radiation patterns, were then measured in a semi-anechoic chamber. The measured reflection coefficient showed less than -10 dB in the entire WiBro band (2.3 GHz \sim 2.4 GHz). Fig. 4 shows the measured and simulated radiation pattern of the single antenna (Ant. 1) that was placed at the left side of the rear window at 2.35 GHz. The measurement showed -6 dBi average gain and it agrees with the simulation.

To more closely observe the diversity performance, we compared the channel capacity of the proposed antenna to that of monopole-type antennas as shown in Fig. 5. The channel capacity of our antennas with optimal feed locations showed higher value compared to other cases.

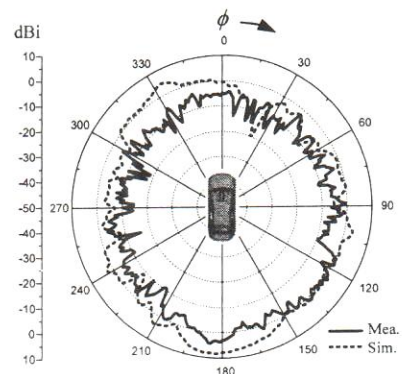


Figure 4. The radiation pattern of the proposed antenna.

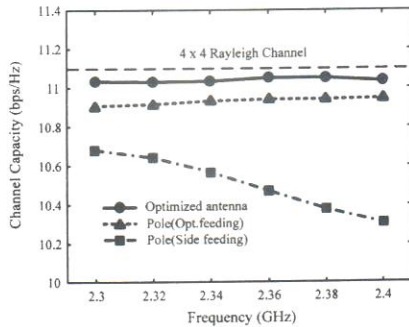


Figure 5. Channel capacity by the antenna structure and feeding point.

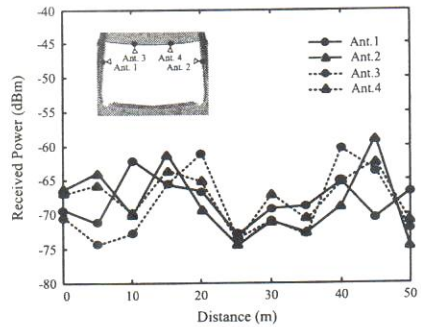


Figure 6. The received power of diversity antennas.

To confirm the diversity performance in a real situation, we measured the received WiBro signal power in an urban environment where multi-path fading exists. The measurement was conducted while we were driving a sedan at 3 km/h. The data was collected using a laptop computer connected to an Agilent 8593A spectrum analyzer by a USB-GPIB controller. Fig. 6 shows the received signal powers from the four antennas. The correlation coefficient between the antennas was calculated as shown in Table II. The result shows a minimum correlation coefficient between Ant. 1 and Ant. 2, and a maximum value between Ant. 2 and Ant. 4. The average correlation coefficient among the four antennas was 0.39.

III. CONCLUSIONS

In this paper, we propose vehicle on-glass diversity antenna for WiBro applications to improve the low radiation gain due to the body blockage effect of the vehicle. We optimized a planar triangular patch structure to step-up the low input resistance of the on-glass antenna. To improve the drivers' field of view, the inside of the triangular patch was partially removed. The proposed antenna was built and antenna characteristics were measured in a semi-anechoic chamber. The measurement showed a matching bandwidth of 11% and an average radiation gain of -6 dBi. The channel capacity using the 3-D radiation pattern of the four antennas was above 11 bps/Hz. The measured correlation coefficients using the WiBro signal strength of the four antennas were less than 0.4. These results verify that the proposed diversity antenna is suitable for use in WiBro application.

TABLE II
CORRELATION COEFFICIENT BETWEEN THE RECEIVED POWERS

Ant. No.	1-2	1-3	1-4	2-3	2-4	3-4	Total
Correlation coefficient	0.08	0.31	0.13	0.42	0.77	0.60	0.39

ACKNOWLEDGMENTS

This study was supported by the IT R&D program of MKE/IITA. [2009-F-042-01, A Study on Mobile Communication System for Next-Generation Vehicles with Internal Antenna Array]

REFERENCES

- [1] K. Yang, S. Ou, H. Chen, and J. He, "Multihop peer-communication protocol with fairness guarantee for IEEE 802.16-based vehicular networks," *IEEE Trans. Veh. Technol.*, vol. 56, no. 6, pp. 3358-3370, Nov. 2007.
- [2] Y. Noh, Y. Kim, and H. Ling, "Broadband on-glass antenna with mesh-grid structure for automobiles", *Electron. Lett.*, vol. 41, no. 21, pp. 1148-1149, Oct. 2005.
- [3] R. Abou-Jaoude and E. K. Walton, "Numerical modeling of on-glass conformal automobile antennas," *IEEE Trans. Antennas Propag.*, vol. 46, no. 6, pp. 845-852, Jun. 1998.
- [4] G. J. Foschini and M. J. Gans, "On limits of wireless communications in a fading environment when using multiple antennas", *Wireless Personal Commun.*, vol. 6, no. 3, pp. 311-335, Mar. 1998.
- [5] G. D. Durgin, *Space-time wireless channels*. London: Prentice Hall PTR, 2002.
- [6] Y. Lin and S. Tasi, "Analysis and design of broadside-coupled striplines-fed bow-tie antennas," *IEEE Trans. Antennas Propag.*, vol. 46, no. 3, pp. 459-460, Mar. 1998.
- [7] J. Horn, N. Nafpliotis, and D. E. Goldberg, "A niched Pareto genetic algorithm for multiobjective optimization," in *Proc. IEEE Evolutionary Computation Conf.*, 1994, vol. 1, pp. 82-87.
- [8] L. Dong, H. Choo, R. W. Heath, and H. Ling, "Simulation of MIMO channel capacity with antenna polarization diversity", *IEEE Trans. Wireless Comm.* vol. 4, no. 4, pp. 1869-1873, July 2005.